

# Demonstrating the Elliptical Orbit of Mars using Naked Eye Data

Kevin Krisciunas<sup>1</sup>

## ABSTRACT

Over the course of eleven months we determined the position of Mars on 45 occasions using a handheld cross staff and two to five bright reference stars of known right ascension and declination on each occasion. On average the observed positions are within  $12'$  of the true positions. Given that we took data prior to the start of retrograde motion and well past the end of retrograde motion, we can easily derive the date of opposition to the Sun. We were able to derive the date of perihelion, the orbital eccentricity, and the semi-major axis size of Mars' orbit. We obtain a value of the eccentricity of  $0.086 \pm 0.010$ , which is to be compared to the modern value of 0.0934. Values as low as 0.053 or as high as 0.123 can be rejected at a high confidence level. A simple dataset can be obtained with cardboard and a ruler that demonstrates the elliptical shape of Mars' orbit.

*Subject headings:* Popular Physics, Dynamics - planetary

## 1. Introduction

The fundamental paradigm of solar system astronomy prior to the time of Copernicus was that the Earth was at the center of the solar system. Also, celestial bodies were assumed to move along perfect circles. This led to the system of deferents and epicycles. One prime motivation for the use of epicycles was to account for retrograde motion. Copernicus' great book *On the Revolutions of the Heavenly Spheres* (1543) asserted that the Sun was physically and truly at the center of the solar system, and that this provided a much simpler explanation for the retrograde motion of the planets. However, Copernicus retained circular motion. Also, he retained the notion of epicycles because they were needed to account for variations of distance of the planets from the Sun (Gingerich 1993).

In ancient Greek astronomy, the *direction* towards the Moon, Sun, or a planet was more important than the implied distance to it. Ptolemy's model of the motion of the Moon

---

<sup>1</sup>George P. and Cynthia Woods Mitchell Institute for Fundamental Physics & Astronomy, Texas A. & M. University, Department of Physics & Astronomy, 4242 TAMU, College Station, TX 77843; krisciunas@physics.tamu.edu

implied that its distance from the Earth varied nearly a factor of two. Naked eye observations by this author have demonstrated that without a telescope one can show that the angular size of the Moon varies in a regular fashion, implying that Moon’s distance varies in a regular fashion (Krisciunas 2010). The implied eccentricity of the Moon’s orbit was  $\approx 0.04$ . (The true eccentricity of the Moon’s orbit is 0.055, but its orbit is anything but a simple ellipse, owing to the gravitational force of the Sun.<sup>2</sup>) The point here is that epicycles in Ptolemaic astronomy were a geometrical device to explain retrograde motion (in the case of the planets) or to determine the direction towards the Moon. In Copernicus’ model, the use of an epicycle implies a realistic, physical variation of distance.

In 1609 Johannes Kepler published the original versions of his first two laws of planetary motion: 1) the orbit of a planet is an ellipse, with the Sun at one focus; and 2) what we now call the law of areas, that the radius vector of a planet sweeps out equal areas in equal times. The Second Law can be stated as follows:

$$r^2 d\theta = h, \quad (1)$$

where  $r$  is the distance between a planet and the Sun,  $d\theta$  is an angular increment in radians, and  $h$  is a constant unique to each planet.

Newton’s breakthroughs in mathematics and mechanics led to the realization that Kepler’s First Law needed correction. The very center of the Sun is not at the focus of a planetary orbit. A planet orbits the *center of mass* of the planet-Sun system, and the Sun orbits that center of mass too (Carroll & Ostlie 2007, chapter 2). This idea, of course, has led to the discovery of many extra-solar planets via the radial velocity method.

In the autumn of 2015 Mars was nicely situated in the constellation Leo before sunrise. We began a sequence of observations of Mars using a simple cross staff (Fig. 1).<sup>3</sup>

---

<sup>2</sup>Lahaye (2012) derived a value of the Earth’s orbital eccentricity of  $0.017 \pm 0.001$ , which compares extremely well with the official modern value of 0.0167. This was accomplished by determining the variation of the equation of time (difference of apparent solar time and mean solar time) over the course of the year using observations of the length of the shadow of a *gnomon*. It was also necessary to know the obliquity of the ecliptic, which is directly obtained from such observations on the first day of summer and the first day of winter.

<sup>3</sup>A pattern for making the cross staff can be obtained from this link: <https://sites.google.com/a/uw.edu/introductory-astronomy-clearinghouse/labs-exercises/measuring-angular-sizes-and-distances>. The reader should note that when printed out the scale may look like inches, but the scale is, in fact, somewhat different.

Say the full width of the cross staff is  $d$ , and suppose at a linear distance  $D$  down the ruler the angular separation of two celestial objects exactly matches the width of the cross staff. Then the angular separation of the two objects will be

$$\theta = 2 \tan^{-1} \left( \frac{d}{2D} \right) . \quad (2)$$

If an observer can measure the angular separation of a planet and two stars of known celestial coordinates, there are two solutions for the position of the planet, one on each side of the great circle arc joining the two stars. If the planet is close to being on the great circle arc between the two stars, perhaps no solution results, given errors of measurement. If the positions of a planet and the two stars form a spherical triangle with reasonably equal sides, this is ideal, and the planetary position can be determined as accurately as possible. Because we are using a handheld naked eye instrument, it is advised to use three to five reference stars. We assume a system of accurate stellar coordinates of bright stars along the zodiac. We adopt the J2000.0 coordinates of such stars from the SIMBAD database.

Understanding Johannes Kepler’s efforts to discover the elliptical nature of Mars’ orbit requires serious effort. A good place to start is an article by Gingerich (1989). To make a long story shorter, Kepler believed that an ovoid would fit the (then) most accurate data available (obtained by Tycho and his assistants). Kepler found anomalies amounting to  $8'$  between the measured ecliptic longitudes and his model. Since he believed that Tycho’s data were good to  $\pm 2'$  or better, he concluded that there was a problem with the *model*. This led him to conclude that his *approximation* to the ovoid (namely, an ellipse) was the true orbital shape.

We wondered if it were possible to demonstrate from simple naked eye observations that the orbit of Mars is indeed an ellipse. Or, requiring less rigor, are the positions of Mars consistent with an elliptical orbit? Here we present results based on nearly a year of observations. A full blown orbital determination for the planet Mars is beyond the scope of the present paper. That would involve simultaneously solving for all six orbital elements. We are only trying to show that a data set obtained with simple equipment can be fit with an ellipse of eccentricity  $\approx 0.093$ . Other values of the eccentricity can be shown to give ecliptic longitudes that differ from the observational data by 1.5 deg, far larger systematic differences than the internal random errors of the observations.

## 2. Data Acquisition

In Table 1 we give various data relating to Mars. For each Julian Date we give the “true” right ascension ( $\alpha$ ) and declination ( $\delta$ ) of the planet, obtained using an algorithm by van Flandern & Pulkkinen (1979). These coordinates are accurate to  $\pm 1'$ . Note that these coordinates will correspond to the equinox of date in the years 2015 or 2016. To convert these coordinates to ecliptic latitude ( $\beta$ ) and longitude ( $\lambda$ ) we need the following formulas from spherical trigonometry (Smart 1977, p. 40):

$$\sin(\beta) = \sin(\delta) \cos(\epsilon) - \cos(\delta) \sin(\alpha) \sin(\epsilon) ; \quad (3)$$

$$\sin(\lambda) = \frac{\cos(\delta) \sin(\alpha) \cos(\epsilon) + \sin(\delta) \sin(\epsilon)}{\cos(\beta)} ; \quad (4)$$

$$\cos(\lambda) = \frac{\cos(\delta) \cos(\alpha)}{\cos(\beta)} . \quad (5)$$

$\epsilon$  is the obliquity of the ecliptic,  $23^\circ 26' 21''.406$  for the year 2000. Using the ATAN2 function in FORTRAN or Python with arguments  $\sin(\lambda)$  and  $\cos(\lambda)$ , we obtain the ecliptic longitude in the correct quadrant.

Table 1 also gives the observed right ascension, declination, ecliptic longitude, and ecliptic latitude of Mars derived from the cross staff measurements, along with the number of reference stars used and the value for each date of the Sun’s ecliptic longitude. The values of the Sun’s longitude were calculated using the second method of Meeus (1988, p. 80). This method uses the Sun’s mean anomaly, but apparently does *not* use the Earth’s orbital eccentricity. On occasion we desired one more sufficiently bright reference star and used the *derived* position of Saturn as that reference position.

Consider two celestial objects with equatorial coordinates  $(\alpha_1, \delta_1)$  and  $(\alpha_2, \delta_2)$ . The angular separation ( $\theta$ ) between two objects is:

$$\cos(\theta) = \sin(\delta_1) \sin(\delta_2) + \cos(\delta_1) \cos(\delta_2) \cos(\alpha_1 - \alpha_2) . \quad (6)$$

Next consider a spherical quadrilateral that is bounded by starting and ending right ascensions, and starting and ending declinations. The quadrilateral is divided into a grid, given a nominal increment in each coordinate of 0.01 deg. We used a computer program of our devising that uses the coordinates of two reference stars and the measured angular

distance of a planet from each of these stars to determine the coordinates of the planet. If the coordinates of the stars are J2000.0 coordinates, then the derived right ascension and declination of the planet also have J2000.0 coordinates.

The derived ecliptic coordinates of Mars are shown in Figure 2. The solid line in the plot shows the locus of “true” positions from van Flandern & Pulkkinen (1979). The earliest observations are of lesser quality. On these occasions we only used two reference stars, and was getting used to a new observing procedure. On almost all subsequent occasions we used more than two reference stars. Two of these first three observations are easily shown to be outliers. Our first three observations will thus be excluded from subsequent analysis.

Another thing to note about Figure 2 is that Mars was north of the ecliptic until JD  $\approx$  2,457,504 (April 25, 2016) and then was located south of the ecliptic. In other words, the orbit of Mars is inclined to the ecliptic. The modern value of the orbital inclination is 1.850 deg (Tholen, Tejfel, & Cox 2000, on p. 295). For our purposes here we will assume that Mars’ orbit is coplanar with the ecliptic.

Given that most positions of Mars listed in Table 1 were derived from angular separations with respect to three to five reference stars, almost all derived right ascensions and declinations have easy-to-calculate internal random errors. These are sometimes as small as  $\pm 0.01$  deg (which we do not really believe). On one occasion (JD 2457399.9840) the internal random error for right ascension was  $\pm 0.23$  deg and the internal random error of declination was  $\pm 0.47$  deg. Typical internal random errors for right ascension and declination are  $\sigma_\alpha \approx \sigma_\delta \approx \pm 0.10$  deg.

Since we have “true” positions of Mars from van Flandern & Pulkkinen (1979) we can make a direct estimate of the accuracy of our observations. The easiest way to do this is to precess the ecliptic longitudes from column 4 in Table 1 to equinox J2000 by subtracting 50.25 arc seconds per year times the number of years from JD 2,457,543.5 (January 0.0, 2000) to the date of observation. The ecliptic latitudes require no precession correction. The subsequent differences of ecliptic longitude and latitude (“observed” *minus* “true”) give mean differences of  $-0.062 \pm 0.016$  deg in ecliptic longitude and  $-0.037 \pm 0.027$  deg in ecliptic latitude. The standard deviations of the distributions of differences are:  $\sigma_\lambda = \pm 0.10$  deg and  $\sigma_\beta = \pm 0.17$  deg. The square root of the sum of squares of those errors is  $\pm 0.20$  deg, or  $\pm 12'$ . This is the accuracy of the position of a bright object (such as a planet) obtainable with our simple cross staff.

### 3. Fitting the Data

In Book 5, Chapter 19, of *On the Revolutions of the Heavenly Spheres* Copernicus (1543) derived the perigee, mean, and apogee distances of Mars. He obtained the values 1.374, 1.520, and 1.649 AU, respectively. Thus, Copernicus knew the amount by which Mars’ distance from the Sun varies, and his mean distance is very close to the modern value of the semi-major axis size of Mars’ orbit (1.5237 AU). Further discussion of Copernicus’ model can be found in Appendix A.

Let us consider the elliptical orbit of Mars. The equation of an ellipse is:

$$r = \frac{a(1 - e)}{1 + e \cos \theta} , \quad (7)$$

where  $r$  is the Mars-Sun distance,  $a$  is the semi-major axis of the ellipse,  $e$  is the eccentricity, and angle  $\theta = 0$  when Mars is at perihelion.

The velocity along the orbit (Carroll & Ostlie 2007, Eq. 2.36) is

$$v^2 = G(M_{\odot} + M_{Mars}) \left( \frac{2}{r} - \frac{1}{a} \right) . \quad (8)$$

Since the mass of Mars is  $\approx 3.23 \times 10^{-7} M_{\odot}$  (Tholen, Tejfel, & Cox 2000, p. 295), for our purposes here we shall ignore it.

We wish to calculate the position of Mars at increments of one Earth day starting at the moment of its perihelion. At perihelion  $r = r_{min} = a(1 - e)$ . Using the known semi-major axis size and eccentricity of Mars’ orbit, we can calculate the maximum velocity at perihelion with Equation 8. On perihelion day traveling at velocity  $v_{max}$  Mars moves 0.6349 degrees along its orbit as viewed from the Sun. This allows us to calculate the constant  $h$  for Mars using Equation 1. Then, by alternating use of Equations 7 and 1 we can calculate  $r$  and  $\theta$  for Mars each day along its orbit. The X-Y coordinates are obtained simply:  $X = r \cos(\theta)$  and  $Y = r \sin(\theta)$ .

For the Earth let us adopt a circular orbit. (The eccentricity of the Earth’s orbit is actually about 0.0167.) On average, the Earth moves  $360.0/365.2422 = 0.985647$  degrees per day with respect to the Sun. This gives us another set of X-Y coordinates in the same coordinate system, with the Sun at the origin and the +X-axis in the direction of Mars’ perihelion.

Consider Figure 3. According to the Solar Systems Dynamic Group, Horizons On-Line

Ephemeris System at Jet Propulsion Laboratory, the previous perihelion of Mars occurred on Julian Date 2,457,003.8524 (December 12, 2014, at 08:27:29 UT). The next perihelion occurs on Julian Date 2,457,691.0507 (October 29, 2016, at 13:13:04 UT). For the moment we will take the perihelion dates as given. They are not directly observable, but the date of opposition of Mars essentially is. Mars’ ecliptic longitude differs from that of the Sun by 180 deg near the mid-time of its retrograde motion. From our data we find opposition to have occurred on May 22, 2016, at 2 hours UT. According to the *Astronomical Almanac* for 2016 opposition occurred on May 22nd at 11 hours UT. The agreement is reasonably good.

Mars’ latest opposition occurred 526.9 days after the perihelion of December 12, 2014. Call it 527 days. The X-Y coordinates of the day-by-day position of Mars in our coordinate system give  $\theta = 265.545$  deg on the day of opposition. Since the Earth moves 0.985647 deg per day along its orbit, the 269th pair of Earth coordinates gives an angle  $\theta$  most closely matching that of Mars (265.139 vs. 265.545 deg, in fact). Given the index  $i$  of the Earth’s coordinates, the corresponding index of Mars’ coordinates for the same day is equal to  $i + (527 - 269)$ .

We wrote a simple program in Python that calculates the X-Y coordinates of Mars for each day starting at perihelion, and X-Y coordinates of the Earth. With an appropriate offset of the indices of the two sets of coordinates we can obtain the direction toward Mars *from the Earth* for any given date. Then we can find an arithmetic offset between days-since-Mars-perihelion and Julian Date, and we can find another arithmetic offset to transform the angles obtained to ecliptic longitude. This is just an example of shifting a template in two coordinates to minimize the sum of squares of deviations from the data to the offset template. This produces a goodness of fit parameter. The square root of the goodness of fit parameter divided by the number of data points minus 2 gives the RMS scatter of the fit of the template to the data. Varying the model parameters allows us to search for an even better fit to the data.

Our program lets us generate a template of ecliptic longitude values vs. time. Using the official values of Mars’ perihelion date, orbital eccentricity, and orbit size given in Table 2, we can adjust the X and Y axis values to minimize a goodness of fit parameter and make a plot that fits the data well enough to eye. The goodness of fit parameter is the sum of squares of differences between a template and the data, in other words, like  $\chi^2$  minimization, but with equal weights for all the points.

We wondered if a better fit to our data might be obtained with different fit parameters. In other words, we start by deriving the date of perihelion, using our data. In the top panel of Figure 4 we show the goodness of fit parameter for a range of dates with respect to October 29.5. On the basis of our data, we find the best fit is obtained for a perihelion date of October

25.4. The goodness of fit parameter doubles, compared to the value at the minimum, for perihelion dates October 21.5 and October 29.3. Our perihelion date is therefore October  $25.4 \pm 3.9$ , 2016 (UT). This is the equivalent of December 8.5, 2014 (the date of the previous perihelion). In what follows that is our effective perihelion date, allowing us to work *forward* in time toward the subsequent perihelion on October 25.4, 2016.

How robust is the eccentricity? In the middle panel of Figure 4 we show the goodness of fit parameter for a range of eccentricities ranging from 0.043 to 0.133. The minimum of the sum of squares of residuals occurs for  $e = 0.086$ , with an uncertainty of  $\pm 0.010$ .

Finally, we tried a number of values of the orbital semi-major axis size, ranging from 1.50 to 1.55. The goodness of fit parameter is minimized for  $a = 1.526$  AU. Using our determination of the time of perihelion, the eccentricity, and a slight adjustment to the mean distance from the Sun, we obtain a sum of squares of residuals of 1.111. There were 42 data points used for the analysis, and 2 constraints (adjusting time to truncated Julian Date and adjusting angle to ecliptic longitude). The best fit to our data gives an RMS residual of  $\pm 10'.0$  for the fit of the ecliptic longitudes to the best model. This is only slightly better than the average difference between the data and the “true” values ( $\pm 12'$ ). Ignoring the eccentricity of the Earth’s orbit was not a serious mistake.

In Figure 5 we plot the observed ecliptic longitudes of Mars (for equinox J2000) vs. the Julian Date. Low order polynomial fits to the two stationary points indicate that retrograde motion lasted for 74.1 days. The range of ecliptic longitude between the stationary points was  $15.23 \pm 0.42$  deg. We also show three fits of the data for values of the orbital eccentricity of 0.053, 0.086, and 0.123. Even if this figure is displayed in color, it is difficult to see that the middle locus is better than the other two. In Figure 6 we show the differentials (data *minus* model). Figure 6 clearly shows that the eccentricity cannot be as small as 0.053 or as large as 0.123. In both cases the model differs from the data by 1.0 to 1.5 degrees 190 days before opposition and 70 days after opposition. Given that the individual positions of Mars are good to  $\pm 0.2$  deg on average, values of the eccentricity of 0.053 or 0.123 are strongly rejected by the data.

## 4. Conclusions

In Table 2 we summarize the values derived from our simple dataset based on naked eye observations using a handheld cross staff. For comparison we also give the official (“true”) values based on a much more sophisticated orbital determination using the most modern methods. Admittedly, in science we almost never have the “true” values for comparison.



Typically, we can only calculate our internal random errors and estimate sources of systematic error.

Our value of the orbital eccentricity of Mars ( $0.086 \pm 0.010$ ) compares reasonably well the official modern value (0.0934). While our data are not accurate enough to *prove* that Mars’ orbit is an ellipse, if we fit the data with an ellipse, the eccentricity must be near 0.09. Thus, a dataset based on naked eye observations can be shown to be in strong agreement with Kepler’s First Law.

We made use of the SIMBAD database, operated at CDS, Strasbourg, France.

### A. Comparison of Copernican and Keplerian Loci

In Figure 7 we show Copernicus’ model for the orbit of Mars. He retained the notion of perfectly circular orbits and therefore required an epicycle to account for the known variation of the distance of the planet from the Sun. Here we use a primary circle of radius 1.520 AU and one epicycle. Perihelion is obtained at position  $p$ , when  $r = 1.374$  AU. The epicycle turns around twice for every rotation of the primary circle. The combination gives us a nearly elliptical orbit.

In Figure 8 we compare Copernicus’ two circle solution for Mars with the Keplerian ellipse having  $a = 1.52366$  and  $e = 0.0934$ . The Copernican solution differs from the Keplerian ellipse by as much as 0.027 AU.

## REFERENCES

- Carroll, B. W., & Ostlie, D. A. 2007, *An Introduction to Modern Astrophysics*, 2nd ed., San Francisco: Pearson/Addison-Wesley
- Copernicus, N. 1543, *On the Revolutions of the Heavenly Spheres*, translated by A. M. Duncan, Newton Abbot, London, Vancouver: David & Charles, 1976, pp. 265-266
- Gingerich, O. 1989, in *The General History of Astronomy, Vol. 2, Planetary astronomy from the Renaissance to the rise of astrophysics, Part A: Tycho Brahe to Newton*, R. Taton and C. Wilson, eds., Cambridge: Cambridge Univ. Press, pp. 54-78
- Gingerich, O. 1993, in *The Eye of Heaven: Ptolemy, Copernicus, Kepler*, New York: American Institute of Physics, pp. 193-204

- Krisciunas, K. 2010, *Amer. J. Phys.*, **78**, 834
- Lahaye, T. 2012, arXiv:1207.0982
- Meeus, J. 1988, *Astronomical Formulae for Calculators*, 4th ed., Richmond, Virginia: Willman-Bell
- Smart, W. M. 1977, *Textbook on Spherical Astronomy*, 6th ed., Cambridge: Cambridge Univ Press
- Tholen, D. J., Tejfel, V. G., & Cox, A. N. 2000, in *Allen's Astrophysical Quantities*, 4th ed., A. N. Cox, ed., New York, Berlin, Heidelberg: Springer, pp. 293-313
- Van Flandern, T. C. & Pulkkinen, K. F. 1979, *ApJS*, **41**, 391

Table 1. Mars Data

JD <sup>a</sup>	RA <sub>true</sub> <sup>b</sup>	DEC <sub>true</sub> <sup>b</sup>	$\lambda^c$	$\beta^d$	RA <sub>obs</sub>	DEC <sub>obs</sub>	$\lambda_{obs}$	$\beta_{obs}$	N <sup>e</sup>	$\lambda_{\odot}$
313.9757	166.2509	7.3301	164.508	1.335	166.36	7.67	164.48	1.69	2	204.771
322.9604	171.3656	5.2083	170.019	1.365	171.98	4.29	170.94	0.76	2	213.712
329.9688	175.3095	3.5410	174.291	1.387	177.03	3.69	175.81	2.21	2	220.717
338.9674	180.3206	1.4016	179.737	1.413	180.31	1.68	179.62	1.67	2	229.748
344.9931	183.6448	−0.0205	183.353	1.430	183.35	0.10	183.03	1.42	4	235.817
346.9708	184.7339	−0.4856	184.538	1.435	184.58	−0.26	184.31	1.59	2	237.812
359.9819	191.8332	−3.4881	192.243	1.467	191.65	−3.57	192.11	1.32	4	250.977
364.9833	194.5444	−4.6133	195.173	1.477	194.12	−4.34	194.68	1.57	3	256.053
370.9813	197.7750	−5.9320	198.651	1.488	197.45	−5.95	198.36	1.35	4	262.149
373.9674	199.3779	−6.5758	200.370	1.492	199.19	−6.50	200.17	1.49	4	265.187
380.9542	203.1074	−8.0433	204.351	1.501	203.01	−8.09	204.28	1.42	4	272.301
387.9889	206.8359	−9.4620	208.301	1.507	206.51	−9.44	207.99	1.41	4	279.469
391.9813	208.9367	−10.2376	210.512	1.509	208.73	−10.12	210.28	1.55	4	283.538
399.9840	213.1084	−11.7237	214.870	1.508	212.89	−11.56	214.61	1.59	4	291.694
406.9861	216.7061	−12.9424	218.591	1.503	216.45	−12.77	218.30	1.59	4	298.986
410.9840	218.7332	−13.6022	220.672	1.497	218.60	−13.08	220.39	1.95	5	302.894
415.9944	221.2445	−14.3918	223.235	1.488	220.94	−14.19	222.89	1.59	4	307.990
425.9861	226.1101	−15.8320	228.149	1.460	225.91	−15.74	227.94	1.50	5	318.128
429.9715	227.9932	−16.3574	230.034	1.445	227.85	−16.34	229.90	1.43	5	322.164
435.9937	230.7561	−17.0962	232.782	1.417	230.26	−17.05	232.31	1.34	5	328.250
443.9931	234.2464	−17.9769	236.225	1.369	233.84	−17.98	235.85	1.28	5	336.312
449.9799	236.6977	−18.5632	238.626	1.322	236.20	−18.77	238.21	1.02	5	342.326
451.9677	237.4743	−18.7441	239.383	1.305	236.99	−19.08	239.01	0.88	5	344.318
467.9639	242.9168	−19.9740	244.661	1.114	242.59	−20.01	244.37	1.02	5 <sup>f</sup>	0.280
472.9521	244.2518	−20.2824	245.949	1.033	243.94	−20.39	245.68	0.88	5 <sup>f</sup>	5.228
480.9486	245.9309	−20.7106	247.572	0.874	245.74	−20.76	247.40	0.80	5 <sup>f</sup>	13.132
499.9549	247.1279	−21.4551	248.792	0.316	246.72	−21.55	248.43	0.16	4	31.773
512.9493	245.2332	−21.7269	247.097	−0.235	244.72	−21.72	246.63	−0.31	5	44.407
515.9406	244.4834	−21.7551	246.416	−0.381	244.07	−21.62	246.01	−0.31	5	47.304
538.6354	236.5451	−21.4892	239.126	−1.564	236.29	−21.59	238.92	−1.72	5 <sup>f</sup>	69.160
547.6240	233.4845	−21.2476	236.295	−1.979	233.11	−21.32	235.97	−2.13	3	77.768
555.6153	231.4404	−21.0834	234.404	−2.282	231.00	−21.20	234.03	−2.50	5	85.406
564.6441	230.1675	−21.0421	233.243	−2.541	229.98	−20.87	233.03	−2.42	5	94.022
569.6226	229.9735	−21.1049	233.084	−2.648	229.67	−21.42	232.89	−3.03	5	98.770
576.6399	230.3070	−21.3033	233.436	−2.760	230.12	−21.13	233.22	−2.64	5	105.460
582.6149	231.1228	−21.5684	234.238	−2.825	230.94	−21.37	234.02	−2.68	5	111.158
591.6299	233.1991	−22.1097	236.242	−2.880	232.79	−22.22	235.90	−3.08	5	119.759
597.6517	235.0988	−22.5434	238.054	−2.891	234.89	−22.38	237.83	−2.78	4 <sup>f</sup>	125.512
602.6056	236.9372	−22.9283	239.795	−2.889	236.56	−23.13	239.50	−3.16	5 <sup>f</sup>	130.249

Table 1—Continued

JD <sup>a</sup>	RA <sub>true</sub> <sup>b</sup>	DEC <sub>true</sub> <sup>b</sup>	$\lambda$ <sup>c</sup>	$\beta$ <sup>d</sup>	RA <sub>obs</sub>	DEC <sub>obs</sub>	$\lambda_{obs}$	$\beta_{obs}$	N <sup>e</sup>	$\lambda_{\odot}$
624.6229	247.6334	−24.6631	249.743	−2.783	247.18	−24.45	249.30	−2.64	5	151.392
633.5979	252.9637	−25.2414	254.615	−2.707	252.55	−25.30	254.25	−2.81	5	160.063
639.5740	256.7638	−25.5420	258.065	−2.649	256.41	−25.57	257.75	−2.71	5	165.857
646.5729	261.4329	−25.7851	262.284	−2.575	261.01	−25.79	261.90	−2.60	5	172.665
653.5681	266.2981	−25.8906	266.667	−2.494	266.05	−25.93	266.45	−2.54	5	179.495
660.6153	271.3719	−25.8399	271.236	−2.407	270.84	−26.06	270.76	−2.62	5	186.403

Note. — Except for the columns 2 and 10, all values are measured in degrees. A text file containing the data, along with similar data for Venus, Jupiter, and Saturn, can be obtained via <http://people.physics.tamu.edu/public.html/planets.txt>.

<sup>a</sup>Julian Date minus 2,457,000.

<sup>b</sup>True right ascension and declination for equinox of date, using algorithm of van Flandern & Pulkkinen (1979). Accurate to  $\pm 1'$ .

<sup>c</sup>True ecliptic longitude for equinox of date. To compare column 4 values to those in column 8, the column 4 values must be precessed to equinox J2000.0 by subtracting roughly  $0.23^\circ$  (50.25 arc seconds per year).

<sup>d</sup>True ecliptic latitude. These can be compared directly with the values in column 9, without any precession.

<sup>e</sup>Number of reference stars used.

<sup>f</sup>One of the reference “stars” used was Saturn, based on the position *derived* from our observations.

Table 2. Comparison of Parameters for Mars

Parameter	Derived Value	“True” Value
Opposition date <sup>a</sup>	May 22.1	May 22.46 <sup>b</sup>
Perihelion date <sup>a</sup>	October $25.4 \pm 3.9$	October 29.5507 <sup>c</sup>
Orbital eccentricity	$0.086 \pm 0.010$	0.09341233 <sup>d</sup>
Semi-major axis size	1.526	1.52366231 <sup>d</sup>

<sup>a</sup>UT Date and fraction. Year = 2016.

<sup>b</sup>*The Astronomical Almanac for the Year 2016*, p. A3

<sup>c</sup>JPL Solar System Dynamics Group, Horizons On-Line Ephemeris System.

<sup>d</sup>Tholen, Tejfel, & Cox (2000).

Fig. 1.— The cross staff. The cardboard cross piece slides up and down the yardstick. Using simple geometry we can use this device to determine the angular separation of objects in the sky.

Fig. 2.— Positions of Mars in the ecliptic system, as derived from cross staff observations. The solid line is based on a low precision planetary model good to  $\pm 1'$  (van Flandern & Pulkkinen 1979). The yellow dots are test data obtained using only two reference stars. They will be excluded from further analysis.

Fig. 3.— The outer locus represents the orbit of Mars. The dashed X-axis lies along the major axis of Mars’ ellipse. The inner locus represents the orbit of the Earth, which is assumed to be a perfect circle. Mars was observed to be at opposition on May 22, 2016. Here we adopt a date of perihelion for Mars of October 25.4, 2016. The Sun is at the center of the Earth’s orbit, and is at one focus of the Martian ellipse. Mars’ perihelion position is labeled “p”.

Fig. 4.— Fits to observed ecliptic longitudes, solving for desired quantities. *Top:* Using  $a = 1.5237$  AU and  $e = 0.0934$ , we plot the goodness of fit parameter vs. the number of Earth days with respect to October 29.5, 2016 (UT). The best fit is obtained for October 25.4 UT. *Middle:* Using our value for the date of Mars’ perihelion and  $a = 1.5237$  AU, we try various values of the orbital eccentricity. The goodness of fit parameter for our dataset is minimized for  $e = 0.086$ . *Bottom:* Using our value for date of perihelion and  $e = 0.086$ , we try various values of the semi-major axis size. The goodness of fit parameter is minimized for  $a = 1.526$ .

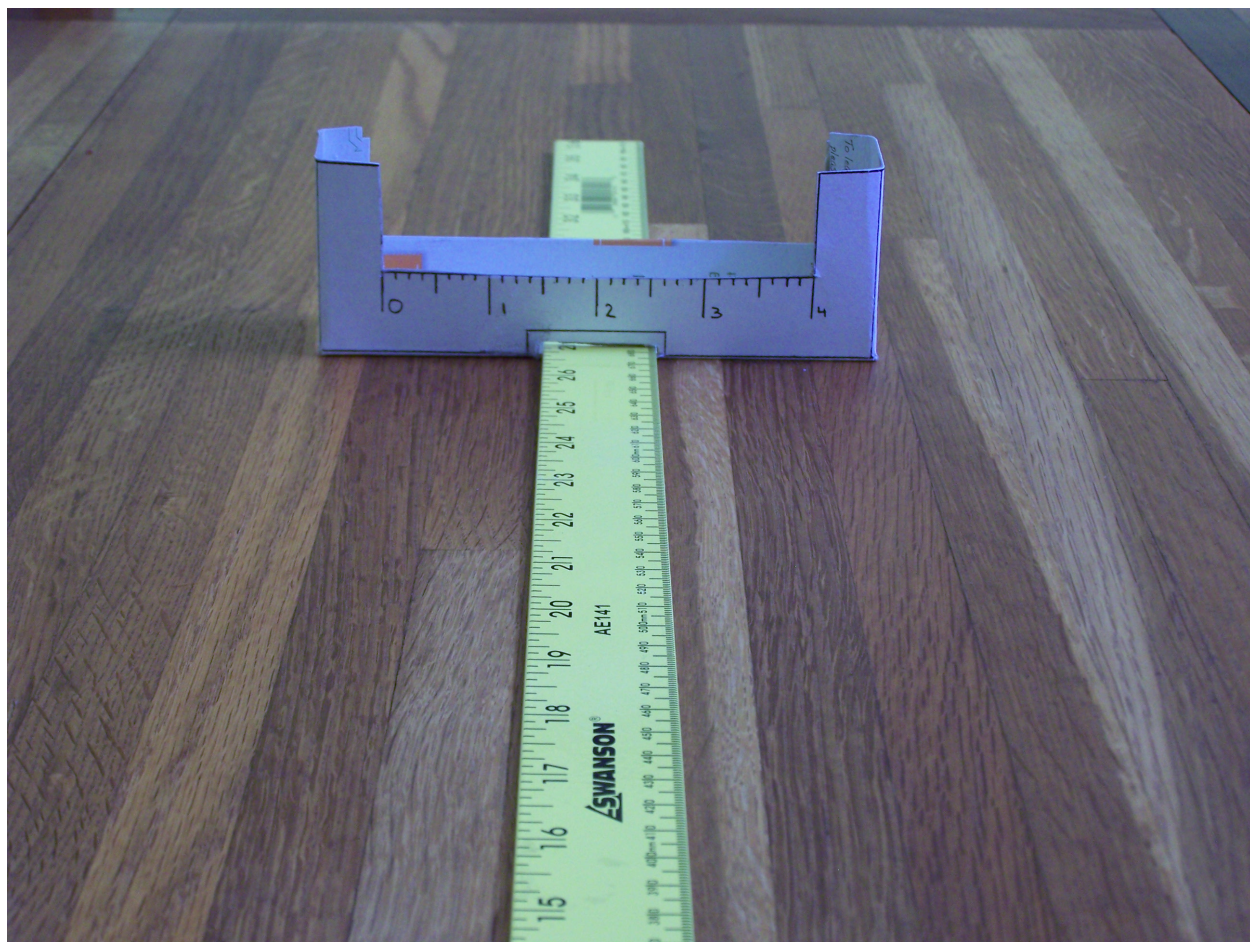
Fig. 5.— The individual data points shown are the observed ecliptic longitudes of Mars from Table 1. The internal random errors are actually much smaller than the size of the points. The three solid lines show the best fits using values of the orbital eccentricity of 0.053, 0.086, and 0.123. The first three data points are for display only. They were not included for fitting the loci.

Fig. 6.— Residuals of fits of the three loci shown in Figure 5. Open circles represent residuals from the best fit (perihelion date October 25.4 UT,  $e = 0.086$ ,  $a = 1.526$  AU). The first three points are for display only. They were not included for any fitting. Triangles are residuals for  $e = 0.053$ , and squares are residuals for  $e = 0.123$ . Clearly, the lowest and highest values of eccentricity lead to residuals as large as  $\pm 1.5$  degrees, considerably larger than the uncertainties of the individual data points (about  $\pm 0.2$  deg).

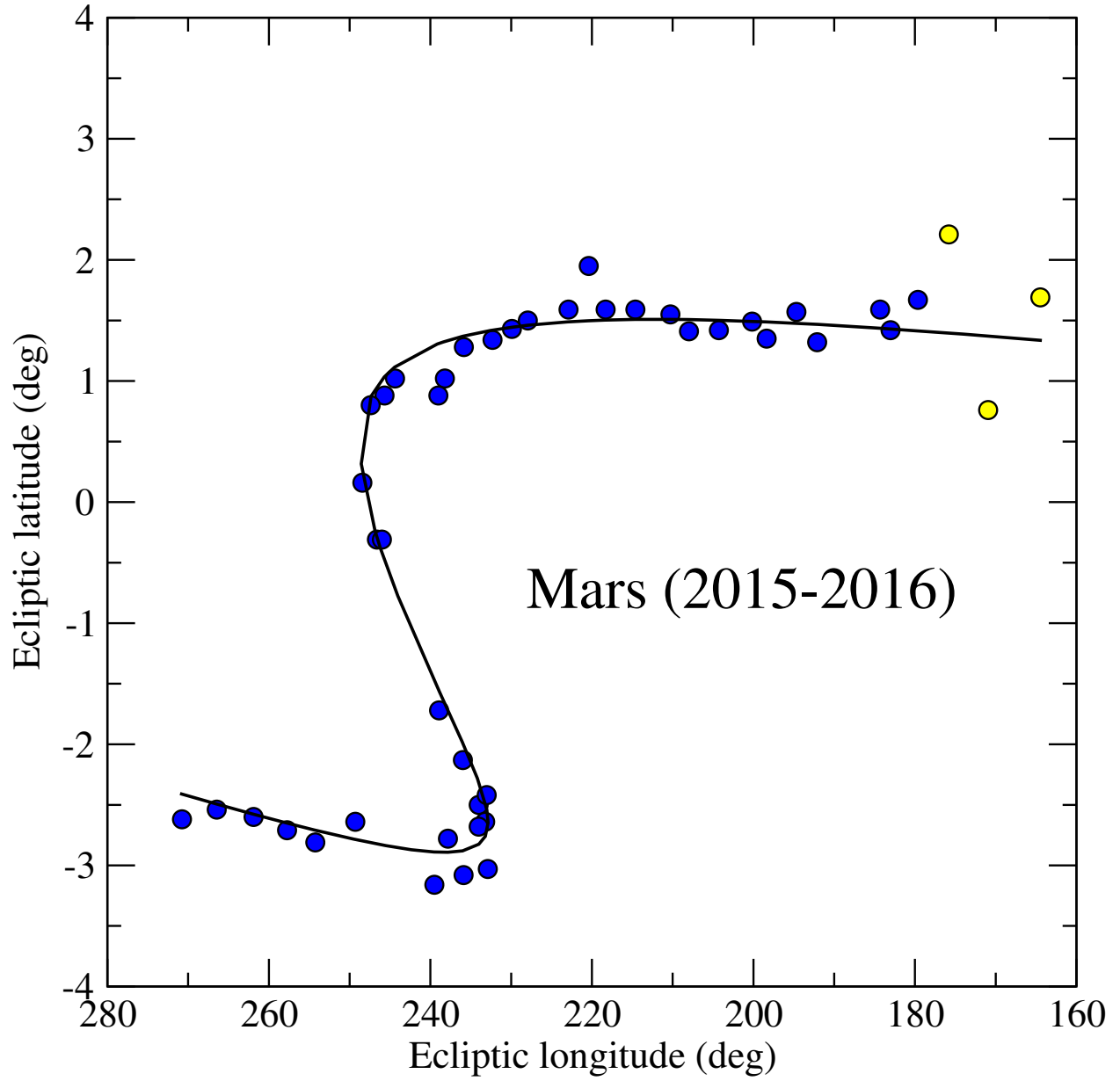
Fig. 7.— The approximation of the orbit of Mars by Copernicus. The Sun is at the center of the larger (blue) circle. The smaller solid circle represents an epicycle that turns around

twice as fast as the larger solid circle. Combining both circular motions gives the dashed (red) line, which is Copernicus’ approximation to the true orbit of Mars around the Sun. Mars’ perihelion position is labeled “p”.

Fig. 8.— Here the outer dashed (red) circle is the model of Mars’ orbit by Copernicus, also shown in Fig. 7. The inner black solid circle is the Keplerian elliptical orbit of Mars shown in Fig. 3. The maximum radial deviation of the Copernican orbit and the Keplerian elliptical orbit is only 0.027 AU. The perihelion position of Mars is labeled “p”.

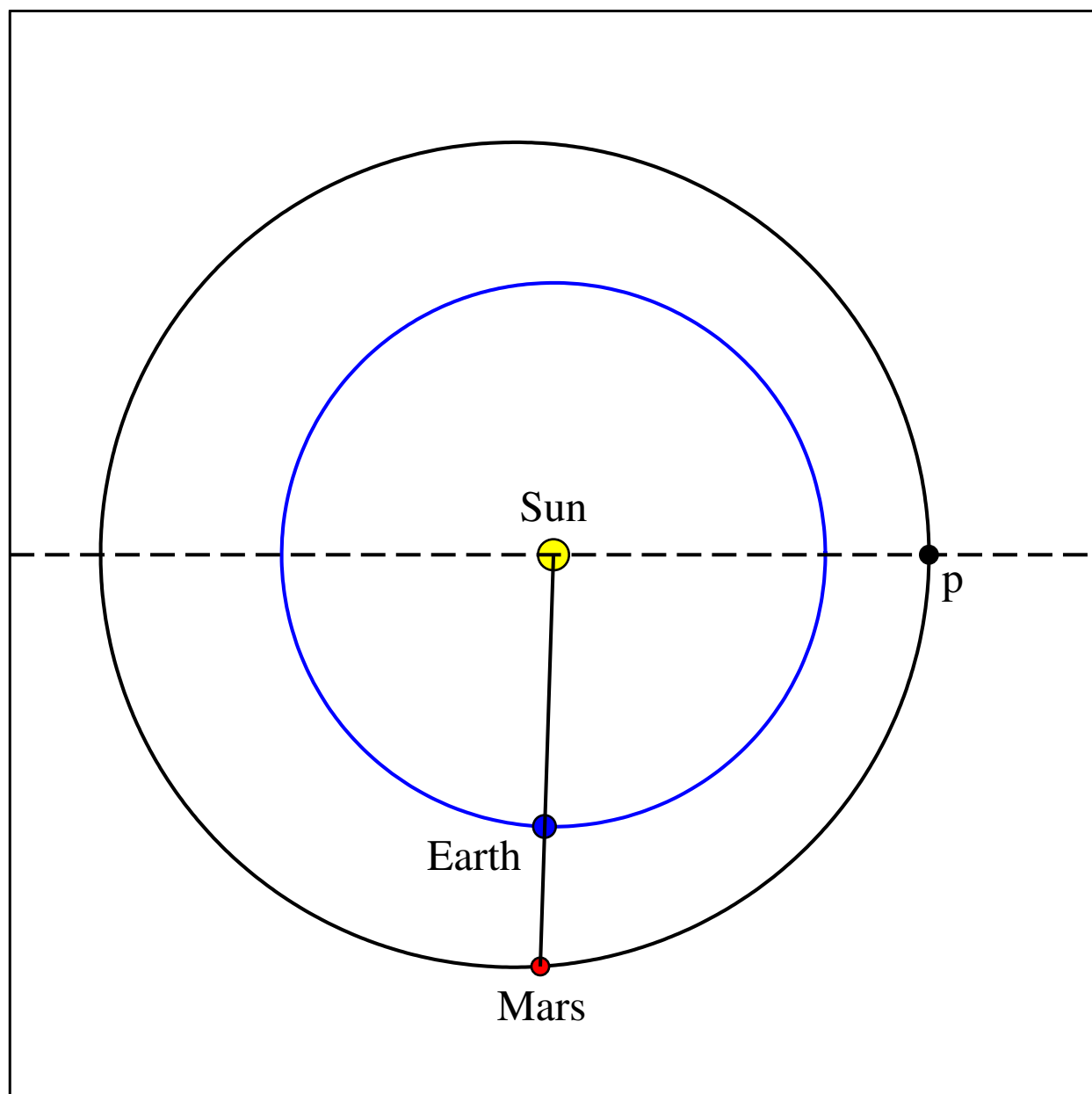


Krisciunas Fig. 1.

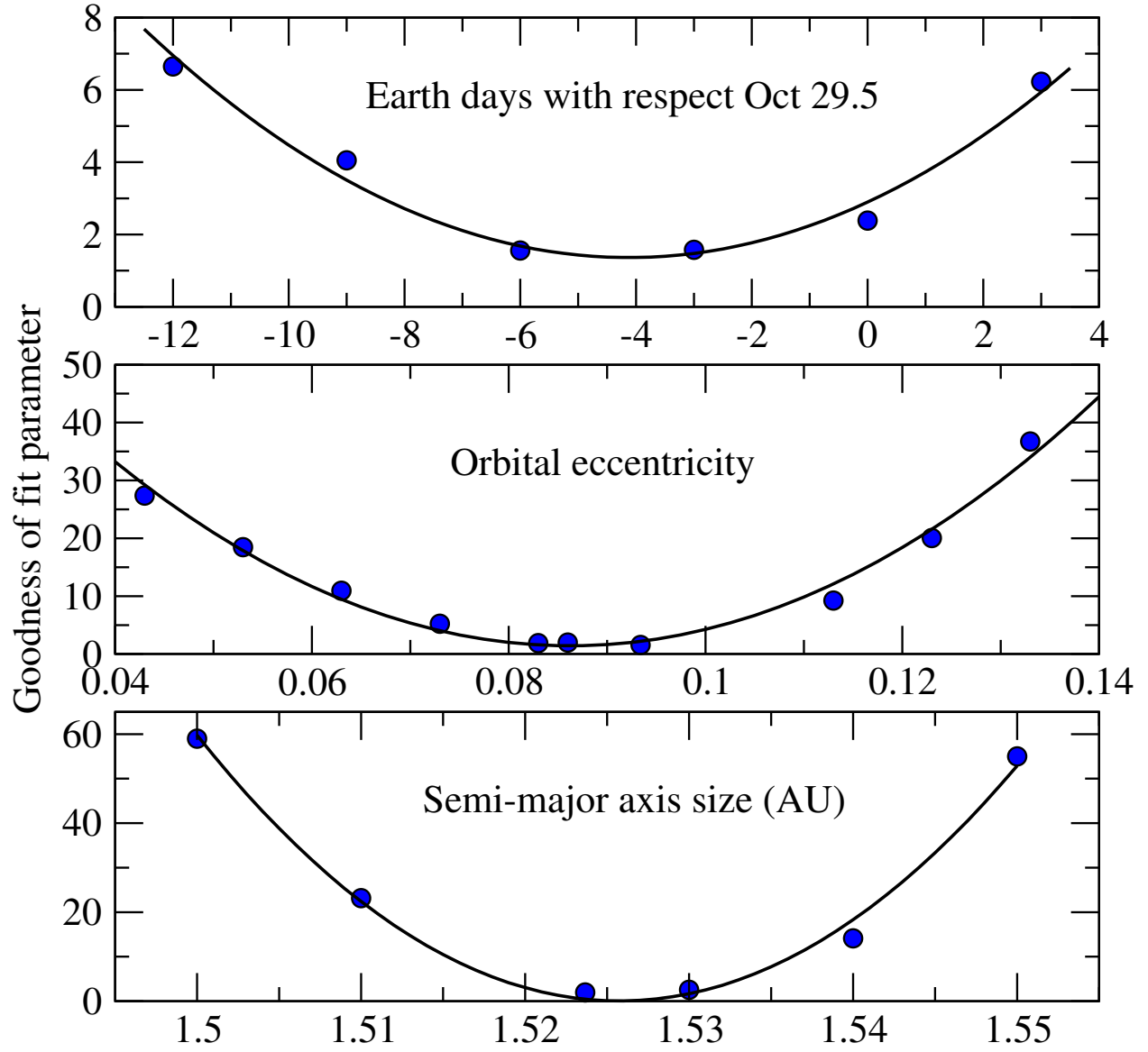


Krisciunas Fig. 2.

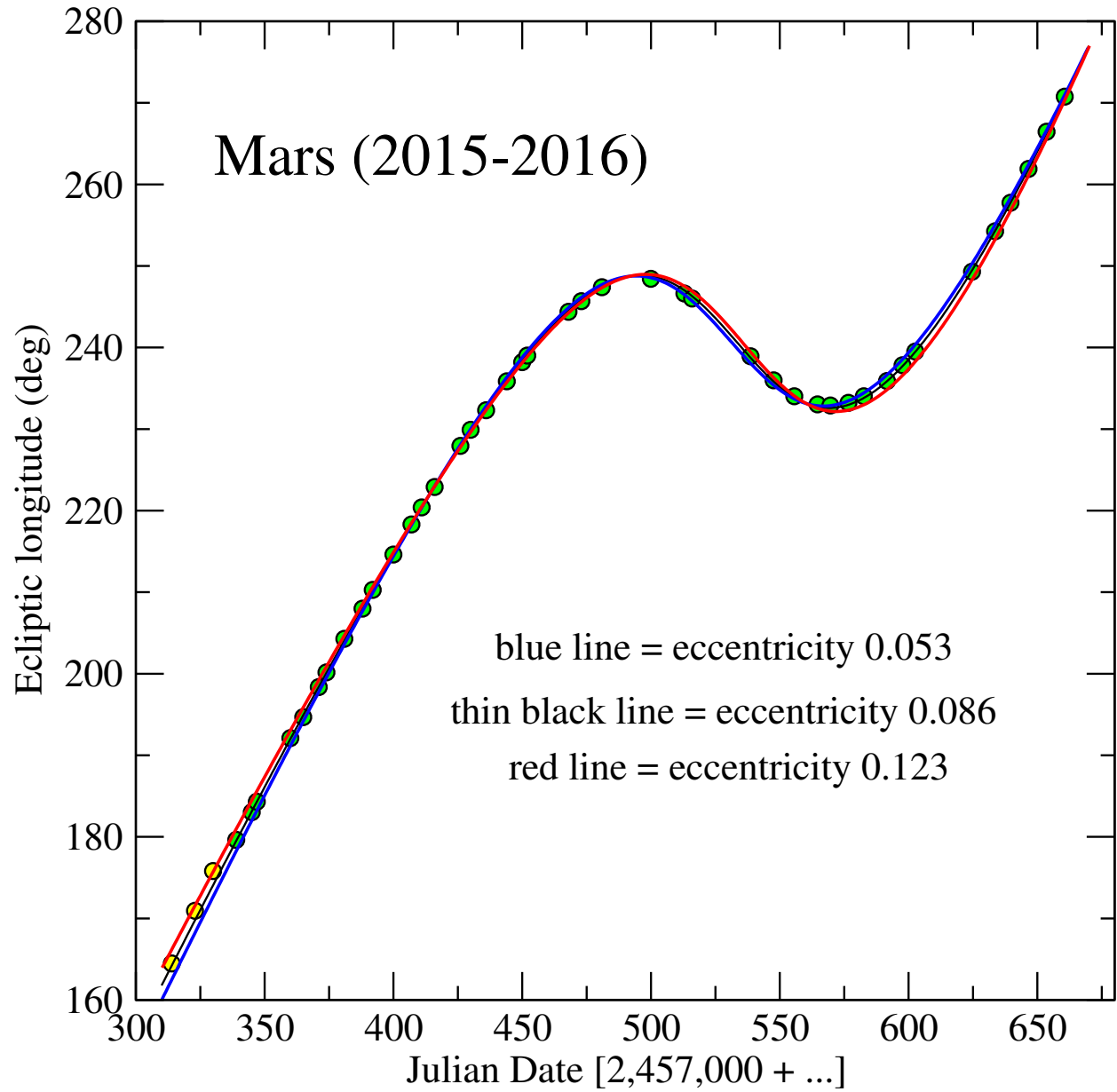




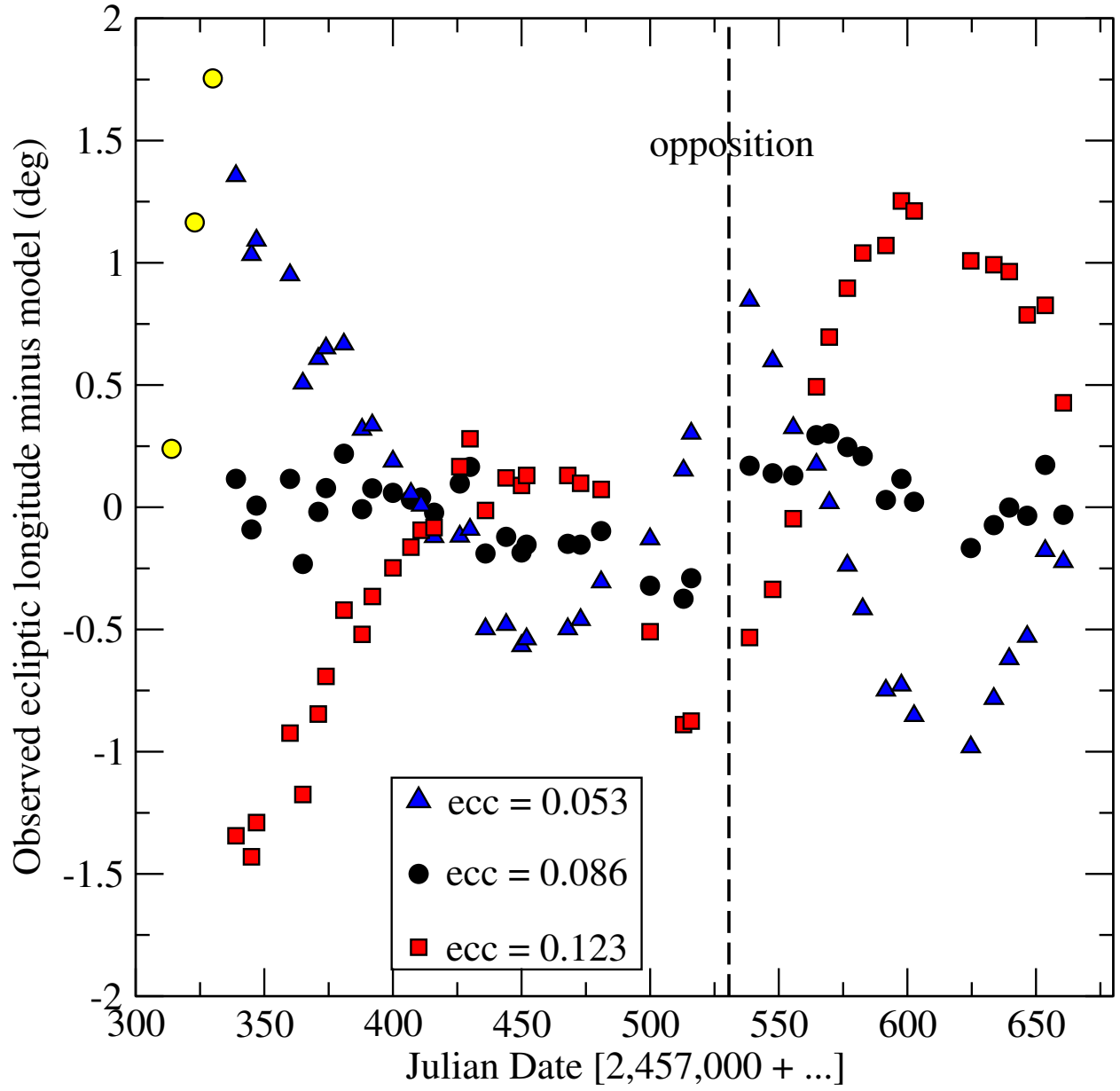
Krisciunas Fig. 3.



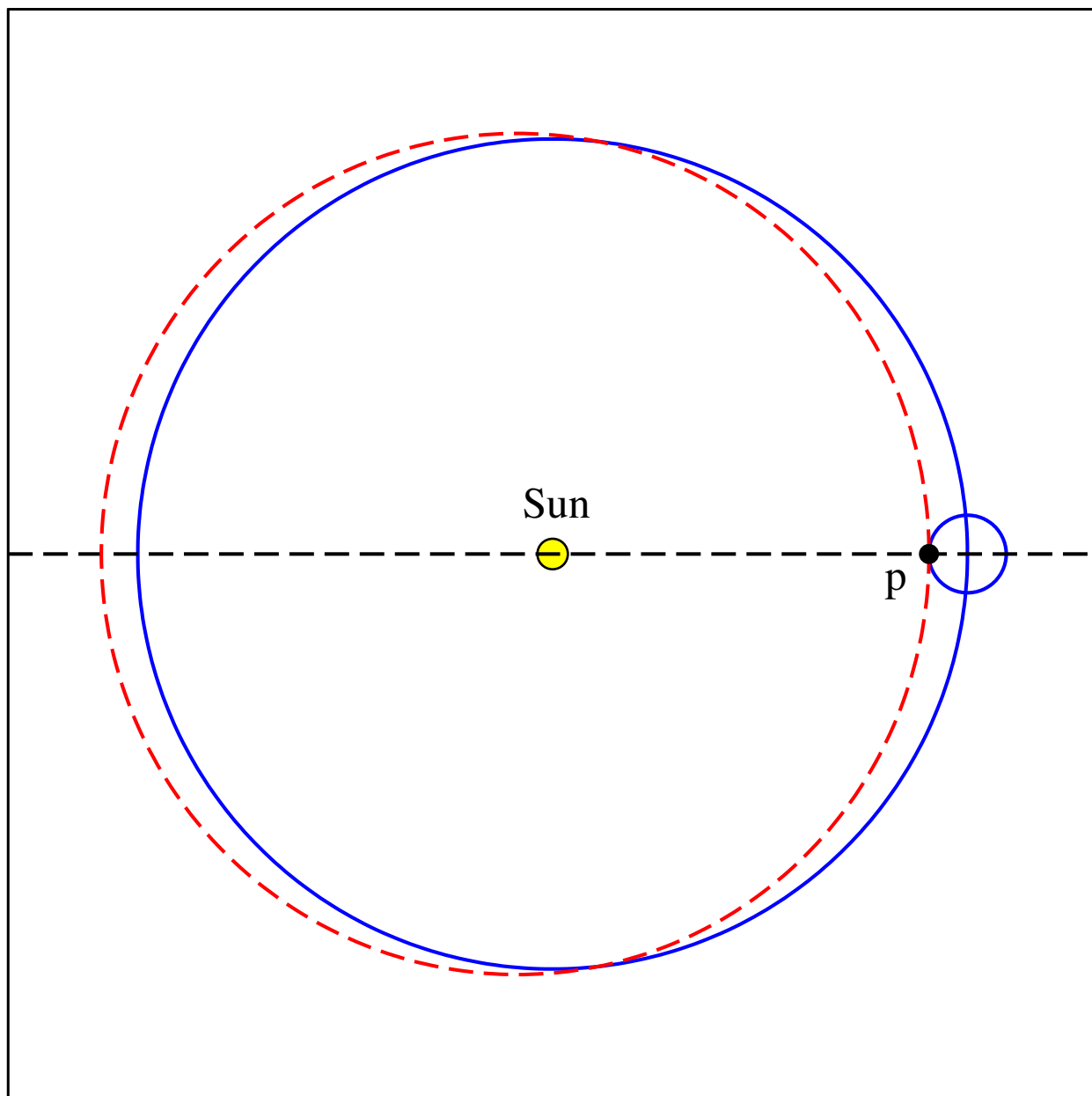
Krisciunas Fig. 4.



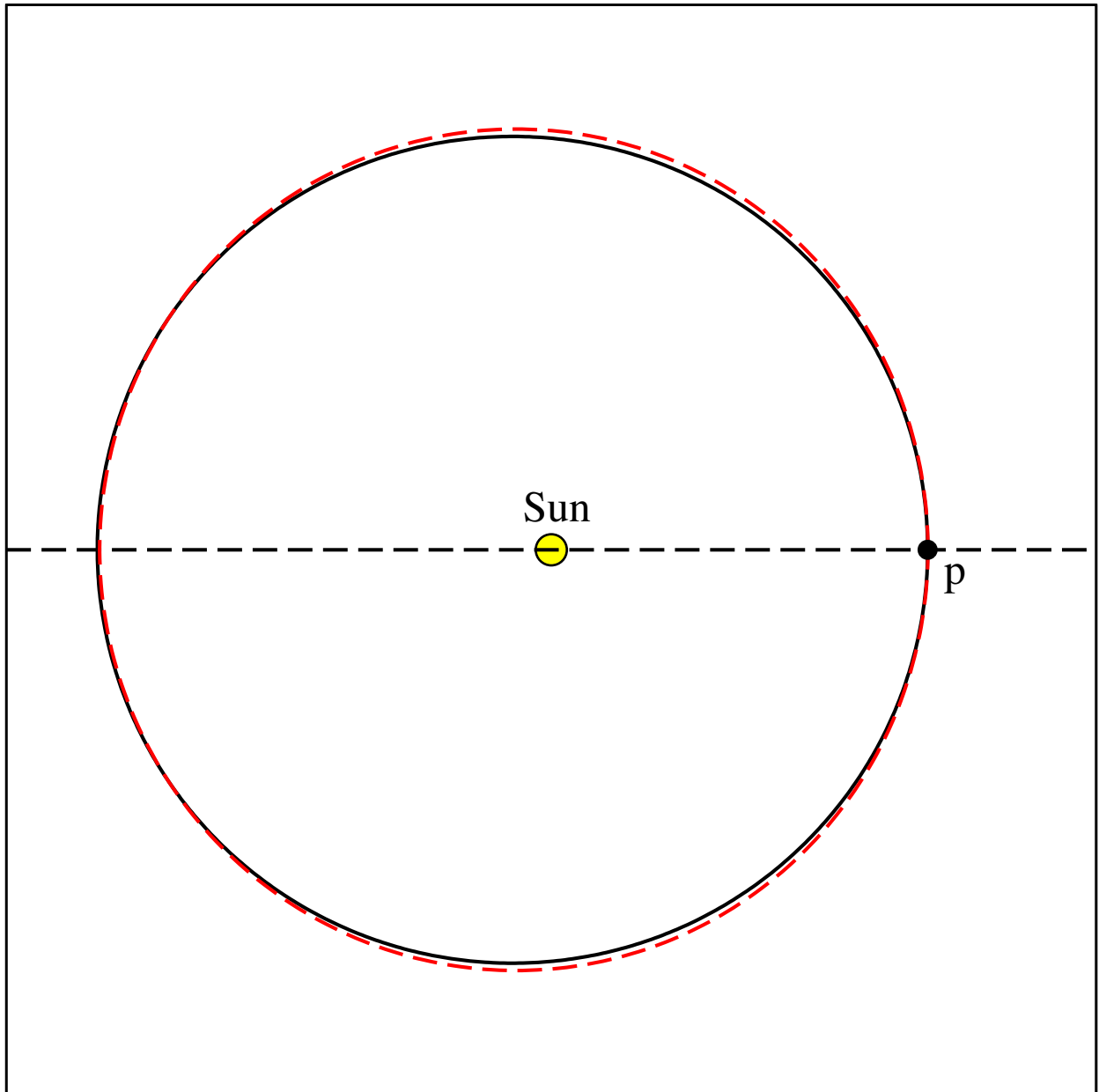
Krisciunas Fig. 5.



Krisciunas Fig. 6.



Krisciunas Fig. 7.



Krisciunas Fig. 8.